

Characterizing cycle structure in complex networks

Tianlong Fan^{1,2}, Linyuan Lü^{1,2,3*}, Dinghua Shi^{4*} & Tao Zhou^{5*}

The ubiquitous existence of cycles is one of important originations of network complexity, as cycle is the simplest structure that brings redundant paths in connectivity and feedback effects in dynamics. Hence the in-depth analyses on cycle structure may yield novel insights, metrics, models and algorithms for network science. By measuring the extent to which a node is involved in other nodes' smallest cycles, this paper proposes an index, named cycle ratio, to quantify the importance of individual nodes. Experimental tests on real networks suggest that cycle ratio contains rich information in addition to well-known benchmark indices, that is, the node rankings by cycle ratio are largely different from rankings by degree, H-index and coreness, while the rankings by the three benchmarks are very similar to each other. Further experiments show that cycle ratio performs overall better than the three benchmarks in identifying critical nodes that maintain network connectivity and facilitate network synchronization.

The last two decades have witnessed an extensive development in network science¹, with research focuses being shifted from discovering macroscopic properties²⁻⁴ to uncovering the functional roles played by microscopic structures, or even individual nodes and links⁵⁻⁷. Scientists have pieced an increasingly clear picture about the functions of specific structures in disparate dynamical processes, such as the roles of different motifs in biological and communication networks⁵, how information and behaviors propagate along a contacting chain⁸, and how a local star structure self-sustains an epidemic spreading process⁹.

Besides extensively studied chain and star structures, cycle is another interesting and significant structure, which is ubiquitous in real networks¹⁰, and plays significant roles in both structural organization and functional implementation. A cycle, also called loop in literature, can be simply defined as a closed path with the same starting and ending node. Recent studies have uncovered the topological properties of cycles, including the distribution of cycles of different sizes in real and artificial networks¹¹⁻¹⁵, the inhomogeneous nature of the evolution of cycle structure in real networks¹⁶, and the effect of degree correlations on the loop structure of scale-free networks¹⁷, as well as the significant roles of the cycle structure in network functions related to storage¹⁸, synchronizability¹⁹ and controllability²⁰. In addition, the organization of cycles can be utilized to characterize individual nodes and links. For example, a measure called clustering coefficient² is based on counting the number of associated triangles (triangle is the cycle with smallest size), which was recently extended to account for the associated cycles with larger

¹ Institute of Fundamental and Frontier Sciences, University of Electronic Science and Technology of China, Chengdu 611731, China. ² Alibaba Research Center for Complexity Sciences, Alibaba Business College, Hangzhou Normal University, Hangzhou 311121, China. ³ Complex Systems Lab, Beijing Computational Science Research Center, Beijing 100193, China. ⁴ Department of Mathematics, Shanghai University, Shanghai 200444, China. ⁵ CompleX Lab, University of Electronic Science and Technology of China, Chengdu 611731, China. * Correspondence and requests for materials should be addressed to L.L. (linyuan.lv@gmail.com), D.S. (shidh2012@sina.com) or T.Z. (zhutou@ustc.edu).

sizes^{10,21,22}, and the effects of the addition of a none-observed link on the local organization of cycles can be used to estimate the likelihood of the existence of this link²³.

Considering a simple network where direction and weight of a link are ignored and self-loops are not allowed, then a cycle is the simplest structure providing redundant paths to all involved node pairs. That is to say, if two nodes belong to a cycle, there are at least two independent paths connecting them. Such redundancy also brings complicated feedbacks in interacting dynamics. Therefore, the in-depth understanding of cycle structure may provide insights and methods on how to maintain the network connectivity under attacks²⁴ and how to regulate interacting dynamics towards predesigned states²⁵.

In this paper, according to the cycle-based statistics, we propose a novel index (named cycle ratio) to quantify the importance of individual nodes. This index is essentially different from known indices and methods⁷, producing a much different ranking of nodes comparing with degree³, H-index²⁶ and coreness²⁷. Extensive experiments on real networks show that the cycle ratio performs better than well-known benchmarks in identifying the most vulnerable nodes under intentional attacks^{28,29} and the most critical nodes in pinning control^{30,31}. Our finding thus has potential applicability in better preventing catastrophic outages in power grids³², enhancing the robustness of financial networks³³, controlling unmanned air vehicles³⁴ and mobile sensor networks³⁵, and so on.

Results

Considering a simple network $G(V, E)$, where V and E are the sets of nodes and links, respectively. The size of a cycle equals the number of links it contains. The cycles containing node i with the smallest size are called the smallest cycles of node i , and the corresponding size is called node i 's girth¹⁹. Denote by S_i the set of the smallest cycles of node i , and $S = \cup_{i \in V} S_i$ the set of all smallest cycles of G , we define the so-called cycle number matrix $C = [c_{ij}]_{N \times N}$ to characterize the cycle structure of G , where $N=|V|$ is the number of nodes in G , and c_{ij} is the number of cycles in S that pass through both nodes i and j if $i \neq j$. If $i = j$, c_{ii} is the number of cycles in S that contain node i . Obviously, C is a symmetric matrix. On the basis of the cycle number matrix, we propose an index, named cycle ratio, to measure a node's importance as

$$r_i = \begin{cases} 0, & c_{ii} = 0 \\ \sum_{j, c_{ij} > 0} \frac{c_{ij}}{c_{jj}}, & c_{ii} > 0 \end{cases}$$

According to the above definition, if a node i doesn't belong to any cycle, its cycle ratio is reasonably set to be zero. When $c_{ii} > 0$, all items in the summation are well defined since $c_{jj} > 0$ if $c_{ij} > 0$. The ratio estimates the importance of node i subject to its participation to other nodes' smallest cycles in S . Note that, in our definition, only smallest cycles in S associated with each node are considered since cycles with larger sizes are usually less relevant to the network functions and to account for all cycles is infeasible for most real networks due to the

tremendous computational complexity²³. Figure 1a presents an example network, and figure 1b shows the corresponding cycle number matrix. The process to calculate the cycle ratio of an example node (i.e., node 1) is also shown in figure 1b. The cycle ratios of all nodes are presented in figure 1c. Three well-known node centralities, degree³, H-index²⁶ and coreness²⁷ (see precise definitions of these indices in Methods), are used as benchmarks for comparison. Their values for this example network are also presented in figure 1c.

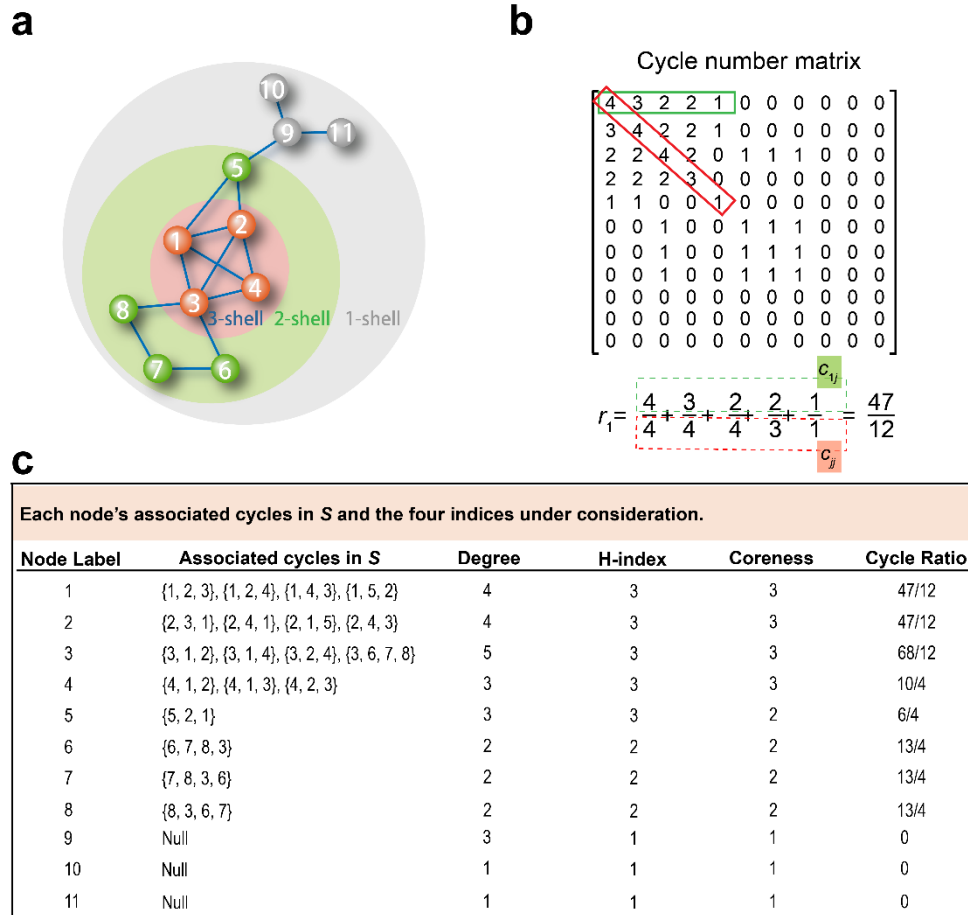


Figure 1. Cycle ratios of nodes in an example network. Plot a is an example network which has three shells according to the k -core decomposition²⁷. Plot b shows the corresponding cycle number matrix and how to calculate the cycle ratio of node 1. Every node's degree, H-index, coreness and cycle ratio are presented in plot c. For this example network, the set of smallest cycles is $S = \{\{1,2,3\}, \{1,2,4\}, \{1,2,5\}, \{1,3,4\}, \{2,3,4\}, \{3,6,7,8\}\}$, and the number of smallest cycles in S is 6.

We test the performance of cycle ratio in identifying vital nodes subject to two well-studied dynamical processes, the node percolation^{28,29} and synchronization²⁵. The former considers nodes' ability to maintain the network connectivity and the latter accounts for nodes' capacity to regulate interacting dynamics towards a certain predesigned state. The experiments are carried out on six real networks from disparate fields, including the neural network of *C. elegans* (*C.elegans*)³⁶, the email communication network of the University at Rovira i Virgili in Spain (Email)³⁷, the collaboration network of jazz musicians (Jazz)³⁸, the collaboration network of scientists working on network science (NS)³⁹, the US air transportation network (USAir)²⁶, and the protein-protein interaction network of yeast (Yeast)⁴⁰. Their basic topological features are summarized in Table 1.

Table 1 | The basic topological features of the six real networks.

Networks	N	M	$\langle k \rangle$	$\langle d \rangle$	c
C.elegans	297	2148	14.46	2.46	0.29
Email	1133	5451	9.62	3.61	0.22
Jazz	198	2742	27.7	2.24	0.62
NS	379	914	4.82	6.04	0.74
USAir	332	2126	12.81	2.74	0.63
Yeast	2375	11693	9.85	5.10	0.31

Here N and M are the number of nodes and links, $\langle k \rangle$ and $\langle d \rangle$ are the average degree and average distance, and c is the clustering coefficient².

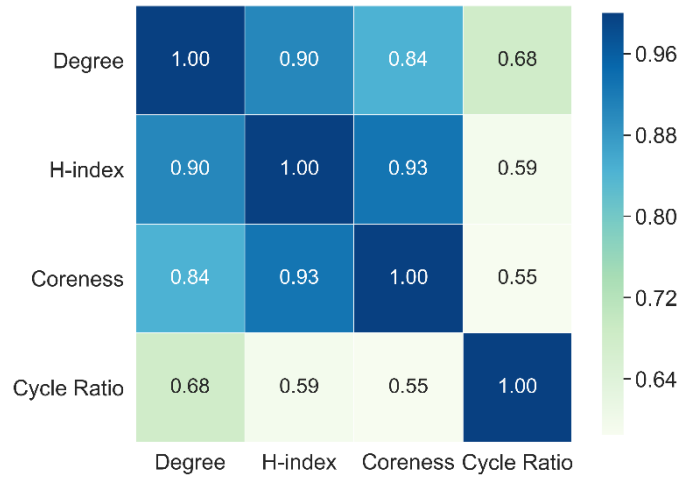


Figure 2. The average correlation matrix for the four indices. Each element is obtained by averaging over the six real networks, and the value is visualized by the color.

Before penetrating into each index's ability to identify dynamically critical nodes, we first see whether cycle ratio contains rich information in addition to the three benchmarks. We apply the Kendall's Tau^{41,42} (τ) to measure the correlation between pairs of indices (see the definition of τ in Methods). Given two indices X and Y , if $\tau(X, Y)$ is close to 1, it indicates that X and Y are highly correlated and less differential to each other. Figure 2 shows the average values of τ between all index pairs over the six real networks (the correlation matrices for all the six networks are shown in Supplementary Section S1), from which one can clearly observe that the correlations between degree, H-index and coreness (~ 0.89) are remarkably higher than the correlations between cycle ratio and the other three (~ 0.61). Therefore, the resulted node rankings produced by degree, H-index and coreness are very similar to each other. That is to say, although the performance of H-index or coreness in some specific tasks is better than degree^{26,27}, the node rankings produced by H-index and coreness contain less information in addition to the one produced by degree, and vice versa. In contrast, as suggested by the lower correlations, the node rankings produced by cycle ratio have rich information in addition to these produced by degree,

H-index and coreness. This is a very important yet easy-to-be-ignored marker about the potential value of a newly proposed index since the lower correlations between the proposed index and known indices indicate a higher potential possibility that the proposed index will provide novel insights beyond known indices.

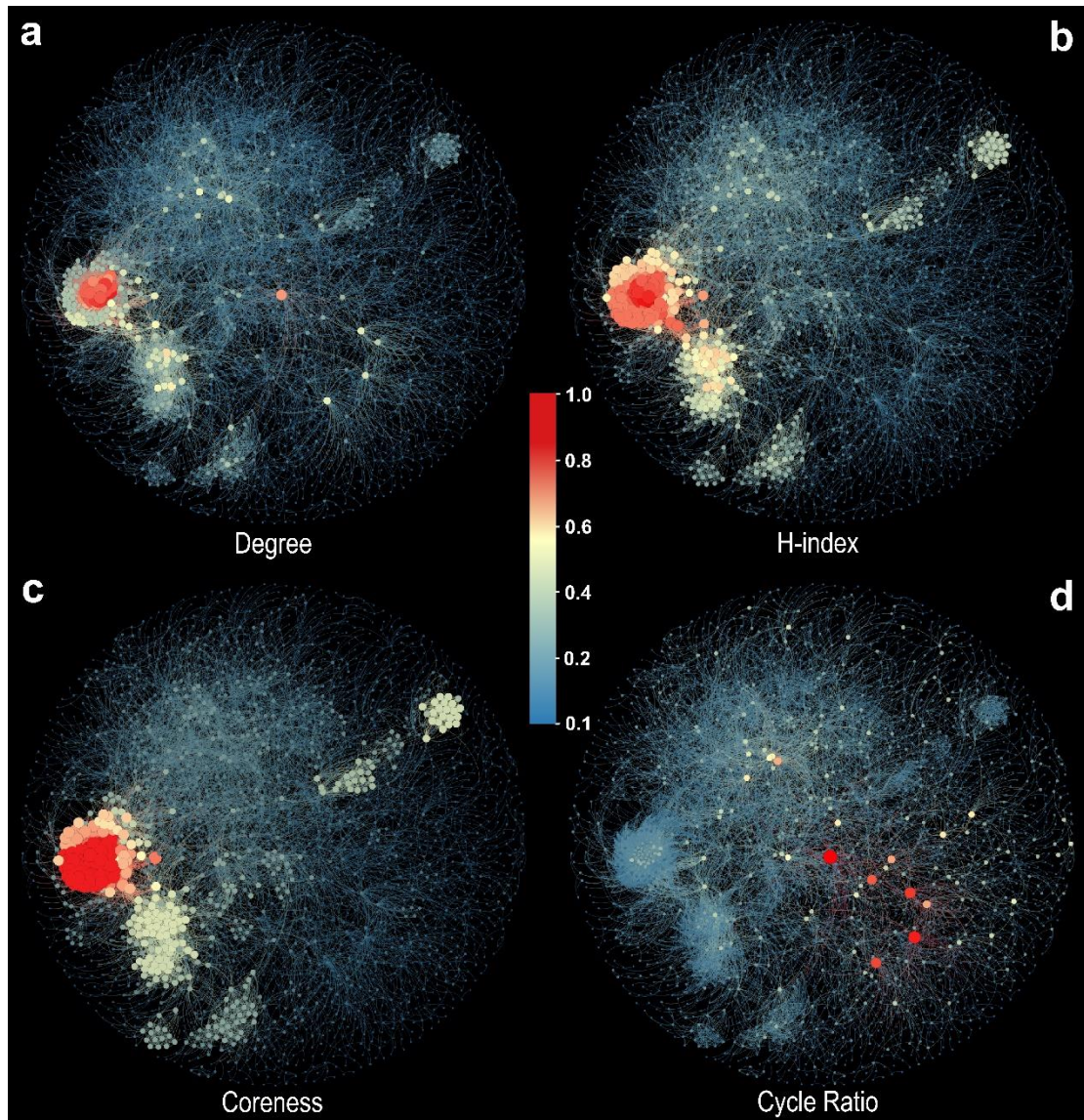


Figure 3. Visualization of the rankings of nodes produced by degree, H-index, coreness and cycle ratio. The Yeast network is taken for example. In each plot, the sizes of nodes are proportional to their values of the corresponding index. The color of a node indicates its relative value normalized by the maximum value. For example, in Plot a, a node i 's relative value is k_i/k_{\max} where k_i is i 's degree and k_{\max} is the maximum degree of Yeast.

Figure 3 presents four visualized networks corresponding to the resulted rankings by the four indices under consideration. Very intuitively, the vital nodes selected by degree, H-index and coreness are highly overlapped, while the ones selected by cycle ratio are much different. Therefore, we believe the in-depth analyses of cycle ratio may uncover novel insights that cannot be obtained by analyzing known node centralities. In addition, as indicated by the centralized

localizations, the vital nodes selected by degree, H-index and coreness are densely connected with each other, in consistent to the so-called rich-club phenomenon^{43,44}. As a contrast, the vital nodes suggested by cycle ratio are more spread with sparser connections among them. This is a significant advantage of cycle ratio if one would like to find out a set of vital nodes, because if the selected vital nodes tend to be clustered to each other, their influential areas will be highly overlapped and thus their collective influences are probably weaker^{27,45,46}.

To evaluate the importance of nodes in maintaining the network connectivity, we study the node percolation dynamics^{28,29}. The metric called Robustness⁴⁷ is used to measure the performance of considered indices. Given a network, we remove one node at each time step and calculate the size of the largest component of the remaining network until the remaining network is empty. The Robustness is then defined as

$$R = \frac{1}{N} \sum_{Q=1}^N \Omega(Q),$$

where the relative size $\Omega(Q)$ is the number of nodes in the largest component divided by N after removing Q nodes. The normalization factor $1/N$ ensures that the values of R of networks with different sizes can be compared. For each index, the nodes are ranked in the descending order and the ones in the top places are removed preferentially. Obviously, a smaller R means a quicker collapse and thus a better performance. Figure 4 shows the collapsing processes of the six real networks, resulted from the node removal by cycle ratio and the other three indices. For the majority of the considered networks, cycle ratio leads to much faster collapse than other indices. Table 2 compares the Robustness R of the four indices, from which one can see that the cycle ratio is overall the best index in identifying the most critical nodes in maintaining the network connectivity.

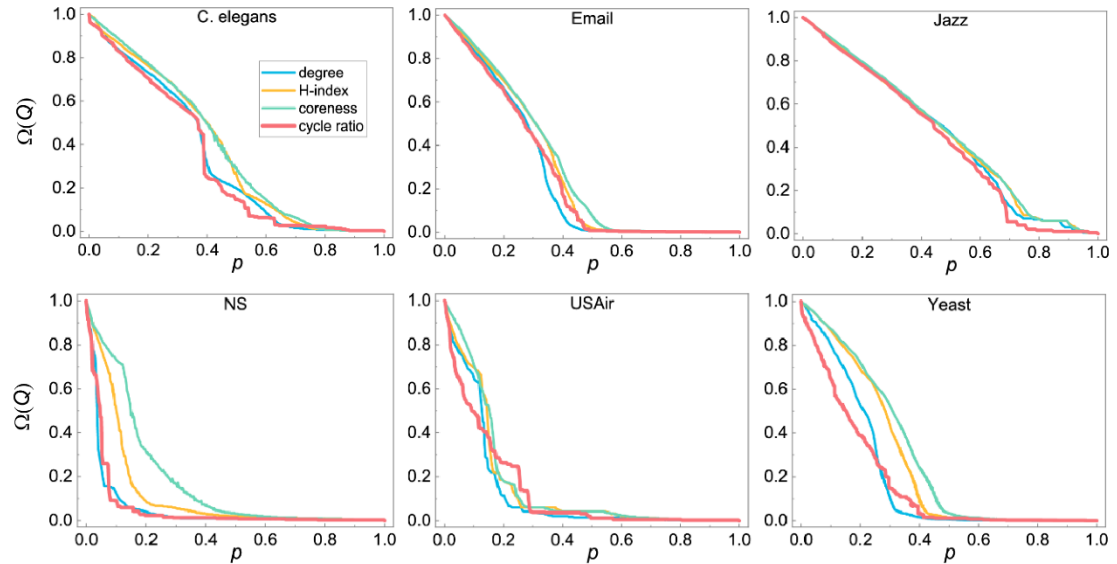


Figure 4. The relative size of the largest component after node removal on the six real networks. The x-axis, $p = Q/N$, is the ratio of removed nodes.

Table 2 | The robustness R of the four indices on the six real networks.

Networks	Degree	H-index	Coreness	Cycle Ratio
C.elegans	0.3303	0.3678	0.3778	0.3167
Email	0.2511	0.2813	0.2949	0.2597
Jazz	0.4394	0.4479	0.4546	0.4190
NS	0.0539	0.1173	0.1803	0.0536
USAir	0.1236	0.1487	0.1587	0.1312
Yeast	0.1960	0.2630	0.2901	0.1726

For each network, the best-performed index is emphasized in bold.

We next evaluate the importance of nodes by measuring the effects caused by pinning these nodes in a synchronizing process^{30,31}. Considering a general case where a simple connected network $G(V, E)$ is consisted of N linearly and diffusively coupled nodes, with an interacting dynamics as

$$\dot{x}_i = f(x_i) + \sigma \sum_{j=1}^N l_{ij} \Gamma(x_j) + U_i(x_1, \dots, x_N),$$

where the vector $x_i \in \mathbf{R}^n$ is the state of node i , the function $f(\cdot)$ describes the self-dynamics of a node, the positive constant σ denotes the coupling strength, U_i is the controller applied at node i , and the inner coupling matrix $\Gamma: \mathbf{R}^n \rightarrow \mathbf{R}^n$ is positive semidefinite. The Laplacian matrix $L = [l_{ij}]_{N \times N}$ of G is defined as follows. If $(i, j) \in E$, then $l_{ij} = -1$; if $(i, j) \notin E$ and $i \neq j$, then $l_{ij} = 0$; if $i = j$, then $l_{ii} = -\sum_{j \neq i} l_{ij}$. The goal of pinning control is to drive the system from

any initial state to the target state in finite time by pinning some selected nodes. Analogous to the node percolation, all nodes are ranked in the descending order by a given index. Then, we successively pin nodes one by one according to the ranking and quantify the synchronizability of the pinned networks, which can be measured by the reciprocal of the smallest nonzero eigenvalue of the principal submatrix^{48,49} (a smaller value corresponds to a higher synchronizability), namely $1/\mu_1(L_{-Q})$, where Q is the number of pinned nodes, L_{-Q} is the principal submatrix, obtained by deleting the Q rows and columns corresponding to the Q pinned nodes from the original Laplacian matrix L , and $\mu_1(L_{-Q})$ is the smallest nonzero eigenvalue of L_{-Q} . Inspired by the metric Robustness, we propose a similar metric named pinning efficiency to characterize the performance of an index subject to pinning control, as

$$P = \frac{1}{Q_{\max}} \sum_{Q=1}^{Q_{\max}} \frac{1}{\mu_1(L_{-Q})},$$

where Q_{\max} is the maximum number of pinned nodes under simulation. Here we set $Q_{\max} = 0.3N$, and we have checked that the choices of Q_{\max} will not affect the conclusion.

Figure 5 shows how $1/\mu_1(L_{-Q})$ decays with increasing number of pinned nodes. Obviously, a faster decay corresponds to a better performance. Table 3 compares the pinning efficiency of the four indices. Similar to the result of the node percolation, cycle ratio is overall the best index in identifying the most efficient nodes in pinning control.

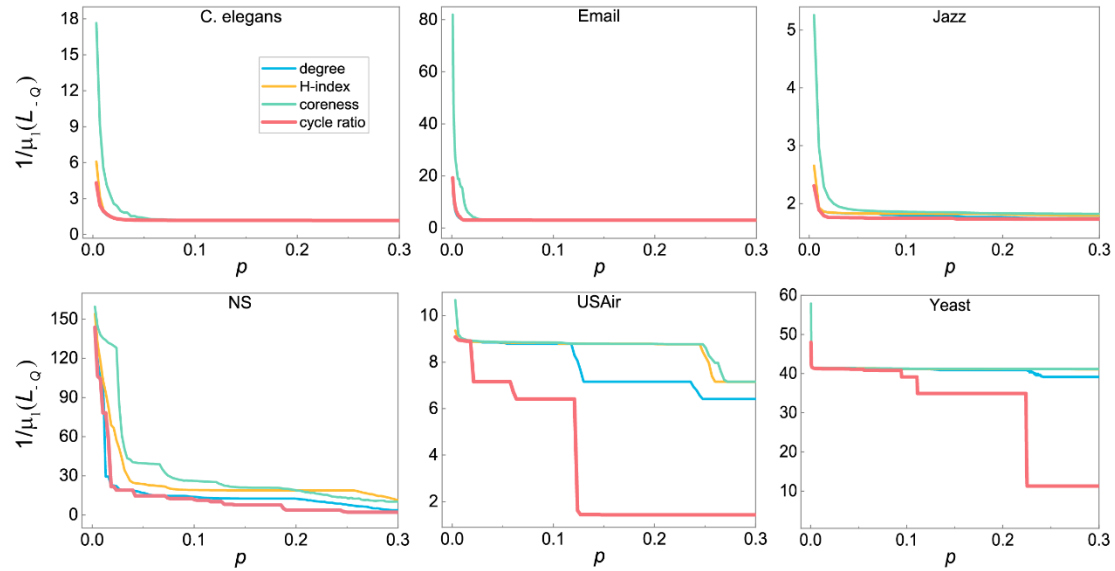


Figure 5. The pinning controllability on the six real networks. The x-axis, $p = Q/N$, is the ratio of pinned nodes.

Table 3 | The pinning efficiency P of the four indices on the six real networks.

Networks	Degree	H-index	Coreness	Cycle Ratio
C.elegans	1.2614	1.2938	1.6490	1.2637
Email	3.1273	3.1445	4.0391	3.1377
Jazz	1.7928	1.8324	1.9368	1.7533
NS	16.1257	25.8633	32.1256	12.9024
USAir	7.6831	8.5382	8.6007	3.6804
Yeast	40.6701	41.2341	41.2826	31.1160

For each network, the best-performed index is emphasized in bold.

Discussion

By analyzing the role of a node in other nodes' local organization of cycles, this paper proposes the index called cycle ratio to measure the importance of individual nodes. Experiments on real networks show that this index outperforms degree, H-index and coreness in identifying vital nodes that are very critical in maintaining the network connectivity and highly efficient in pinning control. A particular advantage of cycle ratio is that it produces much different node rankings from degree, H-index and coreness, and the vital nodes selected by cycle ratio are more spread with sparser connections among them. We believe the in-depth analyses about this index will bring novel insights, metrics, models and algorithms to network science.

An obvious insufficiency of cycle ratio is that it could not be applied for trees or tree-like networks. Even for normal real networks, a fraction of nodes may be not associated with any cycles. These nodes' influences may be different but they are all assigned the same cycle ratio zero. One straightforward way to solve this issue is to combine cycle ratio with some other indices, for example, a mixed index could be $r_i^* = r_i + \varepsilon k_i$ with ε a tunable parameter, hence all the nodes with zero cycle ratio can be ranked by their degrees. Since cycle ratio and degree will produce remarkably different rankings, a subtly designed combination of cycle ratio and degree has the potential to generate much better results than the single index. Similar improvement could also be achieved by combining cycle ratio with H-index or coreness, however, our expected improvement by combining degree, H-index and coreness is lower since they are already very similar to each other. We leave this detailed problem for future study. Another minor issue is that if a network is large and sparse, there may exist a few nodes whose girths are very long and thus to find out the associated smallest cycles are highly time-consuming. Hence in the real implementation, one can set a truncated length and only consider cycles with size no more than it.

We end this paper with two open issues. Firstly, analogous to cycle ratio, making use of cycle structure, one may also design indices to quantify the likelihood of the existence of any unobserved link, which can find applications in solving the link prediction problem. Secondly, the good performance of cycle ratio, as well as the lower correlations between cycle ratio and other benchmark centralities, suggest that the in-depth studies on cycle structure are promising. However, as shown in Supplementary Section S2, both Watts-Strogatz model² and Barabasi-Albert model³ cannot reproduce the cycle-based statistics observed in the real world. We have also tested some other well-known models and none of them can well capture the real statistics. Knowing how cycles are formed may unfold some unknown mechanisms underlying network organization, which is an interesting challenge related to the current work.

Methods

Degree, H-index and Coreness. Degree of a node is the number of its immediate neighbors. *H*-index of a node i is the maximum integer h such that there are at least h neighbors of node i with degrees no less than h . Coreness is obtained by the k -core decomposition⁸. The k -core decomposition process starts by removing all nodes with degree $k = 1$. This may cause new nodes with degree $k \leq 1$ to appear. These are also removed and the process stops when all remaining nodes are of degree $k > 1$. The removed nodes and their associated links form the 1-shell, and the nodes in the 1-shell are assigned a coreness value 1. This pruning process is repeated to extract the 2-shell, that is, in each step the nodes with degree $k \leq 2$ are removed. Nodes in the 2-shell are assigned a coreness value 2. The process is continued until all higher-layer shells have been identified and all nodes have been removed. In the literature, coreness is also referred to as k -shell index.

Kendall's Tau. We consider any two indices associated with all N nodes, $X = (x_1, x_2, \dots, x_N)$ and $Y = (y_1, y_2, \dots, y_N)$, as well as the N two-tuples $(x_1, y_1), (x_2, y_2), \dots, (x_N, y_N)$. Any pair (x_i, y_i) and (x_j, y_j) are concordant if the ranks for both elements agree, namely if both

$x_i > x_j$ and $y_i > y_j$ or if both $x_i < x_j$ and $y_i < y_j$. They are discordant if $x_i > x_j$ and $y_i < y_j$ or if $x_i < x_j$ and $y_i > y_j$. Here n_+ and n_- are used to represent the number of concordant and discordant pairs, respectively. In addition, t_X is the number of the pairs in which $x_i = x_j$ and $y_i \neq y_j$, and t_Y is the number of the pairs in which $x_i \neq x_j$ and $y_i = y_j$. Notice that If $x_i = x_j$ and $y_i = y_j$, the pair is not added to either t_X or t_Y . Comparing all $N(N-1)/2$ pairs of two-tuples, the Kendall's Tau is defined as⁴²

$$\tau = \frac{(n_+ - n_-)}{\sqrt{(n_+ + n_- + t_X) \times (n_+ + n_- + t_Y)}},$$

If X and Y are independent, τ should be close to zero, and thus the extent to which τ exceeds zero indicates the strength of correlation. The above definition of Kendall's Tau⁴² is an improved version of the original definition⁴¹, specifically designed to deal with the case with many equivalent elements.

References

1. Newman, M. E. J. *Networks*. (Oxford University Press 2018).
2. Watts, D. J. & Strogatz, S. H. Collective dynamics of 'small-world' networks. *Nature* **393**, 440–442 (1998).
3. Barabási, A.-L. & Albert, R. Emergence of scaling in random networks. *Science* **286**, 509–512 (1999).
4. Newman, M. E. J. Assortative Mixing in Networks. *Phys. Rev. Lett.* **89**, 208701 (2002).
5. Alon, U. Network motifs: theory and experimental approaches. *Nat. Rev. Genet.* **8**, 450–461 (2007).
6. Lü, L. & Zhou, T. Link prediction in complex networks: A survey. *Physica A* **390**, 1151–1170 (2011).
7. Lü, L. *et al.* Vital nodes identification in complex networks. *Phys. Rep.* **650**, 1–63 (2016).
8. Christakis, N. A. & Fowler, J. H. The spread of obesity in a large social network over 32 years. *N. Engl. J. Med.* **357**, 370–379 (2007).
9. Castellano, C. & Pastor-Satorras, R. Thresholds for epidemic spreading in networks. *Phys. Rev. Lett.* **105**, 218701 (2010).
10. Kim, H.-J. & Kim, J. M. Cyclic topology in complex networks. *Phys. Rev. E* **72**, 036109 (2005).
11. Bianconi, G. & Capocci, A. Number of Loops of Size h in Growing Scale-Free Networks. *Phys. Rev. Lett.* **90**, 078701 (2003).
12. Bianconi, G., Caldarelli, G. & Capocci, A. Loops structure of the Internet at the autonomous system level. *Phys. Rev. E* **71**, 11–14 (2005).
13. Bianconi, G., Gulbahce, N. & Motter, A. E. Local structure of directed networks. *Phys. Rev. Lett.* **100**, 118701 (2008).
14. Rozenfeld, H. D., Kirk, J. E., Bollt, E. M. & Ben-Avraham, D. Statistics of cycles: How loopy is your network? *J. Phys. A* **38**, 4589–4595 (2005).
15. Bonneau, H., Hassid, A., Biham, O., Kühn, R. & Katzav, E. Distribution of shortest cycle lengths in random networks. *Phys. Rev. E* **96**, 062307 (2017).

16. Vázquez, A., Oliveira, J. G. & Barabási, A.-L. Inhomogeneous evolution of subgraphs and cycles in complex networks. *Phys. Rev. E* **71**, 025103 (2005).
17. Bianconi, G. & Marsili, M. Effect of degree correlations on the loop structure of scale-free networks. *Phys. Rev. E* **73**, 066127 (2006).
18. Lizier, J. T., Atay, F. M. & Jost, J. Information storage, loop motifs, and clustered structure in complex networks. *Phys. Rev. E* **86**, 026110 (2012).
19. Shi, D., Chen, G., Thong, W. W. K. & Yan, X. Searching for optimal network topology with best possible synchronizability. *IEEE Circuits Syst. Mag.* **13**, 66–75 (2013).
20. Ruths, J. & Ruths, D. Control profiles of complex networks. *Science* **343**, 1373–1376 (2014).
21. Fronczak, A., Ho, J. A., Jedynek, M. & Sienkiewicz, J. Higher order clustering coefficients in Barabási-Albert networks. *Physica A* **316**, 688–694 (2002).
22. Caldarelli, G., Pastor-Satorras, R. & Vespignani, A. Structure of cycles and local ordering in complex networks. *Eur. Phys. J. B* **38**, 183–186 (2004).
23. Pan, L., Zhou, T., Lü, L. & Hu, C. K. Predicting missing links and identifying spurious links via likelihood analysis. *Sci. Rep.* **6**, 22955 (2016).
24. Albert, R., Jeong Hawoong & Barabási, A.-L. Error and attack tolerance of complex networks. *Nature* **406**, 378–382 (2000).
25. Arenas, A., Díaz-Guilera, A., Kurths, J., Moreno, Y. & Zhou, C. Synchronization in complex networks. *Phys. Rep.* **469**, 93–137 (2008).
26. Lü, L., Zhou, T., Zhang, Q. M. & Stanley, H. E. The H-index of a network node and its relation to degree and coreness. *Nat. Commun.* **7**, 10168 (2016).
27. Kitsak, M. *et al.* Identification of influential spreaders in complex networks. *Nat. Phys.* **6**, 888–893 (2010).
28. Callaway, D. S., Newman, M. E. J., Strogatz, S. H. & Watts, D. J. Network robustness and fragility: Percolation on random graphs. *Phys. Rev. Lett.* **85**, 5468–5471 (2000).
29. Cohen, R., Erez, K., Ben-Avraham, D. & Havlin, S. Breakdown of the Internet under Intentional Attack. *Phys. Rev. Lett.* **86**, 3682–3685 (2001).
30. Wang, X. F. & Chen, G. Pinning control of scale-free dynamical networks. *Physica A* **310**, 521–531 (2001).
31. Li, X., Wang, X. & Chen, G. Pinning a complex dynamical network to its equilibrium. *IEEE Trans. Circuits Syst. I* **51**, 2074–2087 (2004).
32. Albert, R., Albert, I. & Nakarado, G. L. Structural vulnerability of the North American power grid. *Phys. Rev. E* **69**, 025103 (2004).
33. Haldane, A. G. & May, R. M. Systemic risk in banking ecosystems. *Nature* **469**, 351–355 (2011).
34. Tang, Y., Gao, H., Kurths, J. & Fang, J. A. Evolutionary pinning control and its application in UAV coordination. *IEEE Trans. Ind. Informatics* **8**, 828–838 (2012).
35. Ogren, P., Fiorelli, E. & Leonard N. E. Cooperative control of mobile sensor networks: Adaptive gradient climbing in a distributed environment. *IEEE Transactions on Automatic Control* **49**: 1292–1302 (2004).
36. Rossi, R. A. & Ahmed, N. K. The Network Data Repository with Interactive Graph Analytics and Visualization. in *Twenty-Ninth AAAI Conference on Artificial Intelligence* 4292–4293 (AAAI Press, 2015).
37. Guimerà, R., Danon, L., Díaz-Guilera, A., Giralt, F. & Arenas, A. Self-similar community

- structure in a network of human interactions. *Phys. Rev. E* **68**, 065103 (2003).
38. Gleiser, P. & Danon, L. Community structure in Jazz. *Adv. Complex Syst.* **6**, 565 (2003).
 39. Newman, M. E. J. Finding community structure in networks using the eigenvectors of matrices. *Phys. Rev. E* **74**, 036104 (2006).
 40. Jeong, H., Mason, S. P., Barabási, A. L. & Oltvai, Z. N. Lethality and centrality in protein networks. *Nature* **411**, 41–42 (2001).
 41. Kendall, M. G. A new measure of rank correlation. *Biometrika* **30**, 81–93 (1938).
 42. Knight, W. R. A Computer Method for Calculating Kendall's Tau with Ungrouped Data. *J. Am. Stat. Assoc.* **61**, 436–439 (1966).
 43. Zhou, S. & Mondragón, R. J. The rich-club phenomenon in the Internet topology. *IEEE Commun. Lett.* **8**, 180–182 (2004).
 44. Colizza, V., Flammini, A., Serrano, M. A. & Vespignani, A. Detecting rich-club ordering in complex networks. *Nat. Phys.* **2**, 110–115 (2006).
 45. Zhang, J. X., Chen, D. B., Dong, Q. & Zhao, Z. D. Identifying a set of influential spreaders in complex networks. *Sci. Rep.* **6**, 27823 (2016).
 46. Ji, S., Lü, L., Yeung, C. H. & Hu, Y. Effective spreading from multiple leaders identified by percolation in social networks. *New J. Phys.* **19**, 073020 (2017).
 47. Schneider, C. M., Moreira, A. A., Andrade, J. S., Havlin, S. & Herrmann, H. J. Mitigation of malicious attacks on networks. *Proc. Natl. Acad. Sci. U.S.A.* **108**, 3838–3841 (2011).
 48. Liu, H., Xu, X., Lu, J. A., Chen, G. & Zeng, Z. Optimizing Pinning Control of Complex Dynamical Networks Based on Spectral Properties of Grounded Laplacian Matrices. *IEEE Trans. Syst. Man, Cybern. Syst.* DOI: 10.1109/TSMC.2018.2882620, (2018).
 49. Pirani, M. & Sundaram, S. On the Smallest Eigenvalue of Grounded Laplacian Matrices. *IEEE Trans. Automat. Contr.* **61**, 509–514 (2016).

Acknowledgments This work is supported by the National Natural Science Foundation of China (Nos. 11622538, 61673150, 61433014, 11975071), and the Zhejiang Provincial Natural Science Foundation of China (No. LR16A050001). L.L. and T.Z. acknowledge the Science Strength Promotion Programme of UESTC.